Cosmic Masers - from OH to H_0
Proceedings IAU Symposium No. 287, 2012
R.S. Booth, E.M.L. Humphreys & W.H.T. Vlemmings, eds.

doi:10.1017/S174392131200659X

A detailed trace of the pump for 1720-MHz OH masers in SNRs

M. D. Gray

Jodrell Bank Centre for Astrophysics,
School of Physics and Astronomy,
Alan Turing Building, University of Manchester,
Oxford Road, Manchester, M13 9PL, United Kingdom
email: Malcolm.Gray@manchester.ac.uk

Abstract. I have analysed the pumping scheme of 1720-MHz OH masers in great detail.

Keywords. masers, molecular processes, radiative transfer, methods: numerical, stars: winds, outflows, ISM: supernova remnants, radio lines: ISM

1. Introduction

The only OH maser line observed towards supernova remnants (SNRs) is the 1720-MHz outer satellite line from the rovibrational ground state. Only about 10 per cent of Galactic SNRs support 1720-MHz OH masers (see, for example, Hoffman *et al.* (2005)). The SNRs that do support 1720-MHz masers have the following properties: they are old ($>10^4$ yr), placing them in the radiative phase of expansion with non-dissociative C-type shocks expanding at $\lesssim 60\,\mathrm{km\,s^{-1}}$, and they expand into molecular pre-shock gas.

The SNR masers themselves form in the dense post-shock gas, usually in a number of groups (see, for example, Frail & Mitchell (1998)). At VLBI resolution, the brightest maser cores are observed to be elongated parallel to the shock front, as expected, and have scale sizes of order 100 AU. Brightness temperatures of the maser emission from these cores of order 10^8-10^9 K suggest moderate saturation. An example of a maser-supporting SNR is W44, and this object is shown in Fig. 1 with zones of maser emission ringed.

A pumping model was developed by Elitzur (1976), involving radiative transitions and hard-sphere collisions. Large inversions at 1720 MHz could only be produced if excitation to the $^2\Pi_{3/2}, J = 5/2$ rotational state predominated over excitation to rotational states in the $^2\Pi_{1/2}$ ladder, and if the radiative decays to the ground rotational state were optically thick. This situation leads to inversion because the upper state of the 1720-MHz transition, which has $F = 2$, can receive population radiatively from two hyperfine levels in $J = 5/2$ (with $F = 3$ and 2), whilst the lower state, with $F = 1$, can receive population from only one $J = 5/2$ level (with $F = 2$). This pumping model was revisited by Lockett *et al.* (1999), using more modern rate coefficients for collisions between OH and both ortho- and para-H_2, with results that generally supported the earlier hard-sphere model. Large 1720-MHz inversions required the following conditions: $n_{H_2} = 10^4 - 5 \times 10^5\,\mathrm{cm^{-3}}$, $T_K = 50 - 125\,\mathrm{K}$, $T_d < 50\,\mathrm{K}$ and an OH column density of $10^{16} - 10^{17}\,\mathrm{cm^{-2}}$.

2. Computational Model

To make the detailed trace of the population flow, and for comparison with the earlier models introduced above, I obtained an accelerated lambda iteration (ALI) solution to the OH pumping problem in a slab geometry. Apart from a velocity shift of $10\,\mathrm{km\,s^{-1}}$

to simulate the C-shock, the slab was uniform over an extent of 2×10^{16} cm, with the following conditions: $n_{H_2} = 3\times10^4\,\mathrm{cm}^{-3}$, $T_K = 105\,\mathrm{K}$, $T_d = 10\,\mathrm{K}$ and an OH abundance of 10^{-4}. No microturbulence was included: it has a very detrimental effect on the 1720-MHz inversion. Line overlaps were found between the pairs of transitions 6-2, 5-2 and between 8-4, 7-4. See Fig. 2 for the energy level numbering system. The model produced a maximum 1720-MHz inversion of $0.076\,\mathrm{cm}^{-3}$ at a depth of 4.71×10^{14} cm (measured from the side of the slab more remote from the site of the SN).

3. Population Tracing

The population tracing method, implemented through the computer code TRACER, uses a log of matrix operations to restore information usually lost in numerical solutions. For details see Gray (2007) and Gray *et al.* (2005). If the important all-process rate coefficients form a small subset of the total number used in the model (and there is no guarantee of this) then it is often possible to express the inversion derived from a small residual matrix in terms of original coefficients. For example, the 1720-MHz inversion,

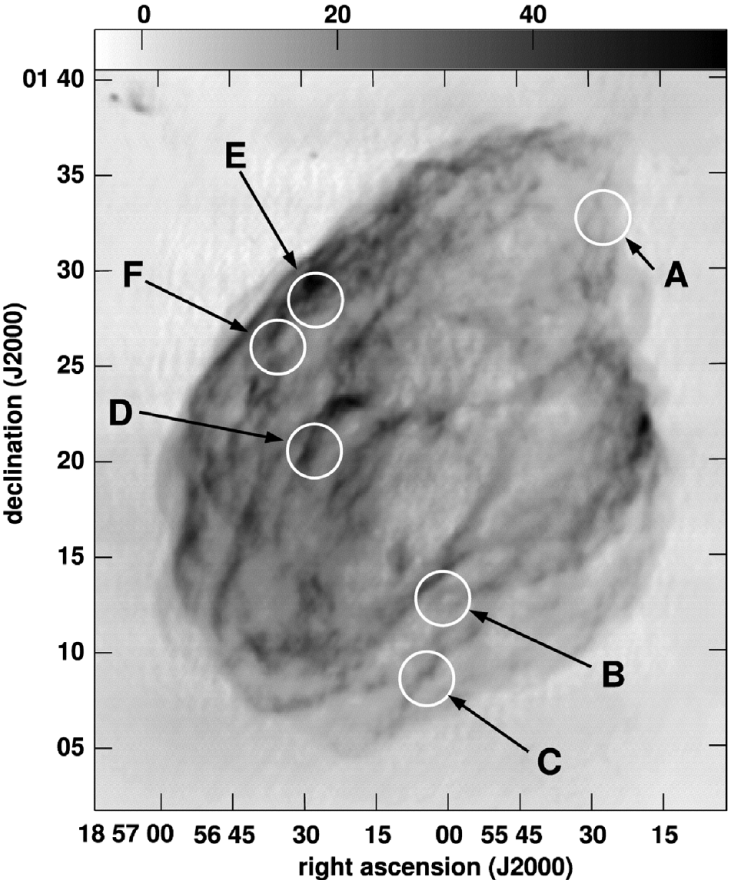

Figure 1. Maser zones (circled) in the SNR W44 superimposed on a continuum image at 1442 MHz (Hoffman *et al.* 2005).

https://doi.org/10.1017/S174392131200659X Published online by Cambridge University Press

expressed in terms of the coefficients of a residual 4×4 matrix is,

$$\Delta\rho_{41} = \frac{N\delta}{Dk_{44}}\left\{\frac{k_{14}}{g_4} - \frac{k_{41}}{g_1} + \frac{k_{33}}{\delta}\left(\frac{k_{12}k_{24}}{g_4} - \frac{k_{42}k_{21}}{g_1}\right) + \frac{k_{22}}{\delta}\left(\frac{k_{13}k_{34}}{g_4} - \frac{k_{43}k_{31}}{g_1}\right) + \frac{k_{12}k_{23}k_{34}}{g_4\delta} - \frac{k_{43}k_{32}k_{21}}{g_1\delta} + \frac{k_{13}k_{32}k_{24}}{g_4\delta} - \frac{k_{42}k_{23}k_{31}}{g_1\delta}\right\} \quad (3.1)$$

where g_x is the statistical weight of level x, $\delta = k_{22}k_{33} - k_{23}k_{32}$ and k_{xy} is the all-process rate coefficient for transfer of population from level x to level y, unless $x = y$, when k_{xx} represents the rate of transfer from level x to all other levels. Note that neither δ nor the expression N/D can change the sign of the inversion. The object of the trace is to expand these coefficients in terms of less-processed forms until the most important coefficients of the original 36×36 matrix are reached.

Note that the rate coefficients are grouped in antagonistic pairs in eq.(3.1), comprising a forward (pumping) term, and a reverse (negative, or anti-pumping) term. I refer to the first of these as the group A set of routes, based on the TRACER expansion of $(k_{14}/g_4) - (k_{41}/g_1)$. Group A routes can only contain levels 1, 4, and levels higher than 4. The next group, B, is the first term in round brackets in eq.(3.1), and is formed of routes that involve levels 1,2,4 and higher levels. The remaining groups are labelled C, D and E in the order that they appear in eq. (3.1).

4. Results

The dominant pumping route found from the trace is shown in Fig. 2; the reverse route is omitted for clarity. Perhaps surprisingly, this route comes from the B-group, involving level 2 as well as levels 1, 4 and the higher levels shown. Apart from the small contribution that pumps via the $^2\Pi_{3/2}, J = 7/2$ levels, the route involves only the ground state and $^2\Pi_{3/2}, J = 5/2$, as expected. The routes shown contribute 63 per cent of the total 1720-MHz inversion under the conditions of the model. The main route comprises three parts: a mainly radiative excitation from level 1 to level 5, followed by a radiative decay to level 2; both these transitions are significantly optically thick, but do not overlap significantly. Finally, excess population in level 2 is moved to level 4 by a rapid collisional transfer across the ground-state lambda-doublet. Additional variations from the B-group involving level 6 and the other half of the $^2\Pi_{3/2}, J = 5/2$ lambda doublet (levels 7 and 8) raise the inverting effect of group B to 84 per cent of the total. The group-D routes, involving level 3 in addition to those involved in B, are also significantly inverting, and, combined with the B-routes, are responsible for over 99 per cent of the inversion. Of the remainder, the A-routes are anti-inverting overall, whilst groups C and E make very small positive contributions to the inversion.

5. Discussion

The traced route in Fig. 2 is similar to that derived from earlier models in that it involves the $^2\Pi_{3/2}$ ladder almost exclusively, and makes particularly strong use of the $J = 5/2$ lambda-doublet. However, it differs in using a radiative excitation and final collisional transfer within the ground-state lambda doublet instead of a collisional excitation to either level 7 or level 8. The basic reason for this is that, under the conditions of the present model, the upward collisional rate coefficients are comparatively slow compared to the radiative excitation rate from level 1 to level 5. For example, the respective fully-traced back first-order collisional rate coefficients for the 1-8 and 1-7 transitions are

https://doi.org/10.1017/S174392131200659X Published online by Cambridge University Press

1.9×10^{-7} Hz and 4.2×10^{-7} Hz. By contrast, the all-process rate-coefficient k_{15}, also fully traced back, is 0.0184 Hz. This leads to an overall pumping rate for the route in Fig. 2 that is of order 50 times faster than those via level 7 and 8, both of which form part of the A-group routes. It should be remembered, however, that the present model is close to the minimum value for overall H_2 number density, and higher densities would make the collisional excitations more efficient. It should also be remembered that the final collisional cross-doublet transfer is faster than the excitation to either level 7 or level 8: k_{24} $=5.72\times10^{-6}$ Hz, but the reverse rate coefficient is the same, so that the necessary predominance of the plotted inverting route and the (omitted) reverse route cannot depend on this final link. In fact, this is borne out by inspecting the groups $k_{15}k_{52}$ and $k_{25}k_{51}$. The former product, part of the pumping route, is the faster because it has the excitation via the stronger transition: 1-5 (which changes F), and the decay via the weaker, taking advantage of the greater optical depth in 1-5, and of the overlap of 5-2 with the stronger 6-2 transition.

6. A more realistic model

The model discussed above, to which TRACER was applied, is a fairly crude representation of a SNR maser zone. In a realistic model, the kinetic temperature, density and OH abundance are likely to vary significantly with depth (that is distance measured from the

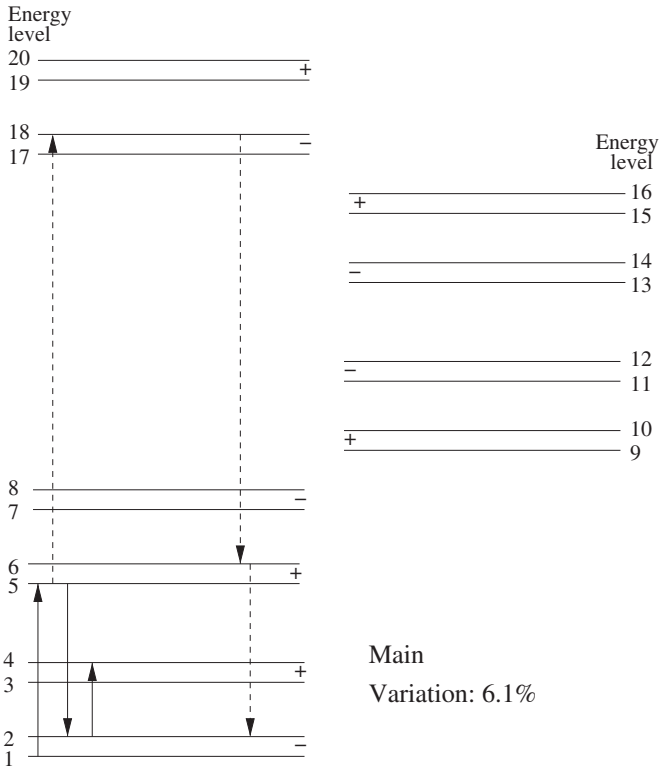

Figure 2. The fastest pumping route for the 1720-MHz inversion. Reverse routes are omitted for clarity. Level numbers are shown, ordered by increasing energy, as are parity designations (+/−). Solid arrows show the main route, whilst the dashed arrows indicate a variation that is effective at the level of 6.1 per cent with respect to the main route.

https://doi.org/10.1017/S174392131200659X Published online by Cambridge University Press

shock front towards the site of the SN). A model that I considered was the set of C-shock solutions by Le Bourlot *et al.* (2002). However, adapting these for the 1720-MHz OH maser system proved problematic because the range of depth where the OH abundance is adequate to form a maser is rather narrow, and has temperatures significantly higher than those associated with 1720-MHz SNR masers.

The remedy is to include the SNR-specific processes of cosmic-ray and X-ray irradiation of the model cloud Wardle (1999). Energetic electrons produced by this irradiation excite H_2 molecules collisionally, with resultant UV-emission. This ultra-violet radiation is sufficient to generate OH from water by photodissociation at large depths, where the temperature is suitable for OH masers to form.

7. Conclusion

A simple model of a SNR maser zone has been constructed, and the pump of the 1720-MHz OH maser in this type of source has been traced in detail. The results are broadly in agreement with earlier work: the pumping routes are almost exclusively confined to the $^2\Pi_{3/2}$ ladder of levels, and to the ground and first excited rotational states in particular. The pump routes rely on radiative decay via optically thick transitions from $J = 5/2$ levels to $J = 3/2$ levels. However, under the single set of conditions so far studied, the initial excitation from level 1 is radiatively dominated, whilst the pump route is completed by a collisional transfer across the arms of the ground-state lambda doublet. This conclusion could change significantly at higher densities where the collisional excitations to $J = 5/2$ are faster.

References

Elitzur, M. 1976, *ApJ*, 203, 124
Frail, D. A. & Mitchell, G. F. 1998, *ApJ*, 508, 690
Gray, M. D. 2007, *MNRAS*, 375, 477
Gray, M. D., Howe, D. A., & Lewis, B. M. 2005, *MNRAS*, 364, 783
Hoffman, I. M., Goss, W. M., Brogan, C. L., & Claussen, M. J. 2005, *ApJ*, 627, 803
Le Bourlot, J., Pineau des Forêts, G., Flower D. R., & Cabrit, S. 2002, *MNRAS*, 332, 985
Lockett, P., Gauthier, E., & Elitzur, M. 1999, *ApJ*, 511, 235
Wardle, M. 1999, *ApJ*, 525, L101

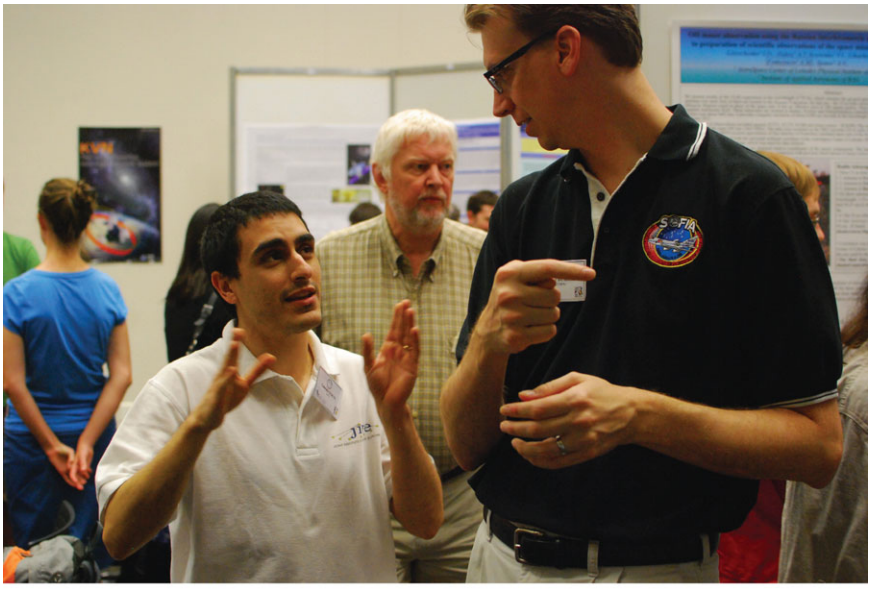

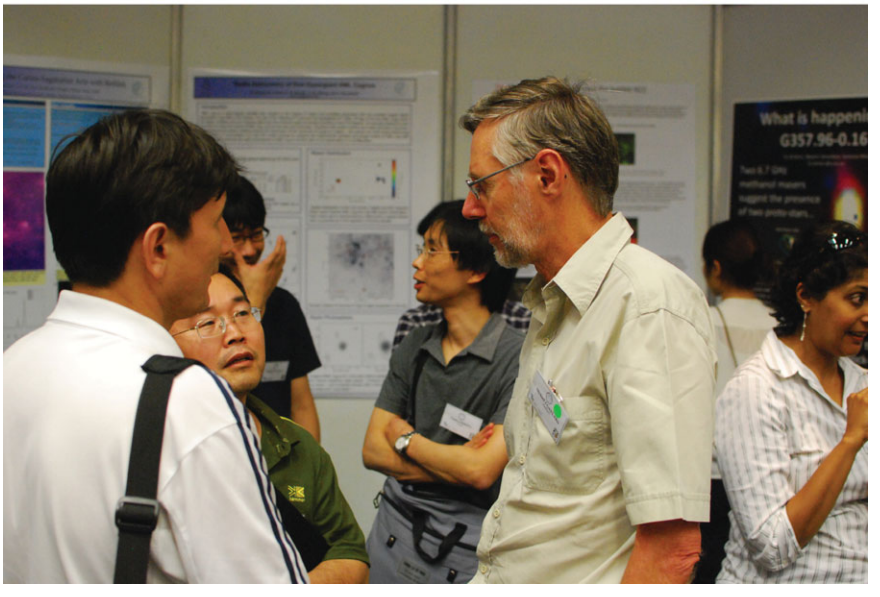

Lively discussions during poster sessions.
Proceeding pictures by Kalle Torstensson.

https://doi.org/10.1017/S174392131200659X Published online by Cambridge University Press